David Gross
Math 164
Prof. Yong
Due 5/2/08 - Turned In 5/11/08

Multi-Domain Spectral Methods to Cure Cancer

1 Problem Background

We are interested in curing cancer with mathematics. To do this, we must focus our efforts and make the correct assumptions. This process was already carried out during the Summers of 2005, 2006, and 2007 and was supported by the National Science Foundation under 3-year grant NSF-DMS-041-4011. We made assumptions before, after, and during we the creation of our model of tumor evolution. Assumptions made before the model is created include that the tumor is avascular, i.e., it has not set up its own blood supply. This means that the effect of the body's blood supply has a much greater effect on the tumor dynamics, which is why we choose to model the immune response to the tumor.

1.1 The Model

1.1.1 The 'Body' or 'Bulk': ODE System

The model consists of a system of ODEs made up of quantities which are dynamic within the system of body, whose quantities are

M_B**:** Chemotherapy drug concentration in the blood, [IU/L]
D_B**:** Dendritic cell concentration in the blood [cells/L]
L_B**:** Antigen-specific activated CD8+ T lymphocytes, [cells/L]

We are concerned with their concentrations in the bulk "compartment" of the body, as the mass-action interactions between populations occurs in many places throughout the body. These interactions are represented by the nonlinear terms in the following differential equations:

$$\frac{dM_B}{dt} = -\omega_{M_B} M_B \tag{1}$$

$$\frac{dD_B}{dt} = \alpha_{D_B} \frac{\langle T \rangle}{\langle T \rangle + k_{D_B}} - \omega_{D_B} D_B - K_{D_B}(1 - e^{-\delta_{D_B} M_B}) D_B \tag{2}$$

$$\frac{dL_B}{dt} = \alpha_{L_B} \frac{D_B}{\zeta_{L_B} + D_B} \frac{L_B}{k_{L_B} + L_B} L_B - u_{L_B} e^{\epsilon_{L_B} D_B} \frac{L_B}{k_{L_B} + L_B} L_B^2 - K_{L_B}(1 - e^{-\delta_{L_B} M_B}) L_B - \omega_{L_B} L_B \tag{3}$$

where

$$\langle T \rangle = \int_0^R \int_0^\pi \int_0^{2\pi} T(r, \phi, \theta) \; d\theta d\phi dr \tag{4}$$

is the integral of tumor density, i.e., the mass of the tumor. The equations that involve this term describe mass-action in a sense that the body has a sense of what size the tumor is that it is fighting. It can then deliver, to the site of the tumor, appropriate chemical levels.

1.1.2 The Tumor Site: PDE System

At the site of the tumor, there are a different set of populations developing:

T**:** Tumor cell density, [cells/mm^3]

$\vec{v}$**:** Tumor cell velocity, [mm/s]

N**:** Nutrient density, [mol/mm^3]

M**:** Chemotherapy drug density, [mg/mm^3]

S**:** Chemical signal responsible for inducing CD8+ T cells to move towards the center of the tumor by chemotaxis, [mol/mm^3]

L**:** Antigen specific CD8+ T lymphocytes, [cells/mm^3]

They follow the system of PDE given below:

$$\begin{aligned}
T_t - \nabla \cdot (\vec{v}T) &= D_T \Delta T + \alpha_T \frac{N}{N+\zeta} T - \omega_T T && (5)\\
&\quad - \frac{(L/T)^\sigma}{s + (L/T)^\sigma} - K_T(1 - e^{-\delta_T M})T && (6)\\
N_t &= D_N \Delta N - \Gamma \frac{N}{N+\zeta} T && (7)\\
M_t &= D_M \Delta M - (\bar{\omega}_M + \gamma T) M && (8)\\
S_t &= D_S \Delta S + \alpha_S - \omega_S S && (9)\\
L_t &= -\mu \Delta S + \Delta L - \omega_L T L - K_L(1 - e^{-\delta_L M})L && (10)
\end{aligned}$$

We assume that there exists an intratumoral pressure $p(r, \theta, \phi, t)$. This pressure exists because the cells inside the tumor boundary are growing faster than the non-cancerous cells outside, and so the cells that are inside are being squeezed into a higher density space. We say that this pressure follows Darcy's Law, that is, for some proportionality constant ν,

$$\vec{v} = -\nu \nabla p. \tag{11}$$

Furthermore, we stipulate that the tumor has constant density, i.e., $T = 1$. We can do this since, for the small tumor sizes we are interested in modeling, the density in the tumor

will diffuse to 1 on a time scale that is much shorter than the development of the tumor. As an aside, we can think that if the pressure builds up enough to have the tumor density be non-constant, the boundary of the tumor will move in such a way as to counteract this density change before is has moved enough to counteract the pressure change. So, choosing this constant density reduces the T PDE to

$$\nu \Delta p = \alpha_T \frac{N}{N+\zeta} - \omega_T - \frac{L^\sigma}{s+L^\sigma} - K_T(1 - e^{-\delta_T M}) \tag{12}$$

and we solve for p instead of both T and $\vec{v}$.

We let the boundary be given by $R = R(\theta, \phi, t)$. To define the time evolution of R, we introduce a moving boundary condition as follows:

$$\left(\frac{\partial R}{\partial t}\vec{u}\right) \cdot \vec{n_R} = \vec{n_R} \cdot \Big(- \nu \nabla p \Big|_{r=R} \tag{13}$$

where novel terms in this equation are defined by

$$\vec{u}(\theta, \phi) = (\cos\theta \sin\phi, \sin\theta \sin\phi, \cos\phi) \tag{14}$$

$$\vec{F} = R\vec{u} \tag{15}$$

$$\vec{n_R} = \frac{\vec{F}_\theta \times \vec{F}_\phi}{\|\vec{F}_\theta \times \vec{F}_\phi\|} \tag{16}$$

Figure 1 represents how this boundary motivation can be visualized.

1.1.3 Linking ODE to PDE

As we linked the PDE to the ODE by integrating the tumor density (which is now equivalent to finding the tumor volume, since the density is constant), we will also link the ODE to the PDE by imposing boundary conditions at the edge of the tumor that correspond with the bulk concentrations:

$$N(R) = N_B \quad L(R) = L_B(t) \quad M(R) = M_B(t) \quad S(R) = 0 \tag{17}$$

$$p(R) = \alpha_\kappa \kappa = \alpha_\kappa \left(\frac{1}{R} - \frac{\mathcal{L}(R)}{2R^2}\right) \tag{18}$$

Note here N_B is constant, but L_B and M_B are functions of time. This is because L_B and M_B are changing in a way that we understand, and we shall incorporate that dependance. The nutrient concentration in the bulk, N_B, is related to diet and overall health, which for the sake of our model we assume is maintainable over the course of treatment. This is not necessarily a valid assumption, however we do not incorporate a model of dietary intake and exercise in our model.

We assume that pressure is proportional to mean curvature $\kappa = \kappa(r, \theta, \phi)$ of the boundary. Here $\mathcal{L}$ is used to denote the angular part of the spherical Laplacian, i.e.,

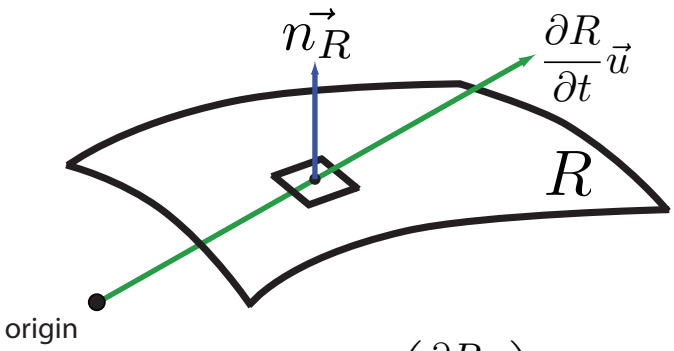

$$\left(\frac{\partial R}{\partial t}\vec{u}\right)\cdot\vec{n_R} = \vec{n_R}\cdot\left(-\nu\nabla p\,\Big|_{r=R}\right)$$

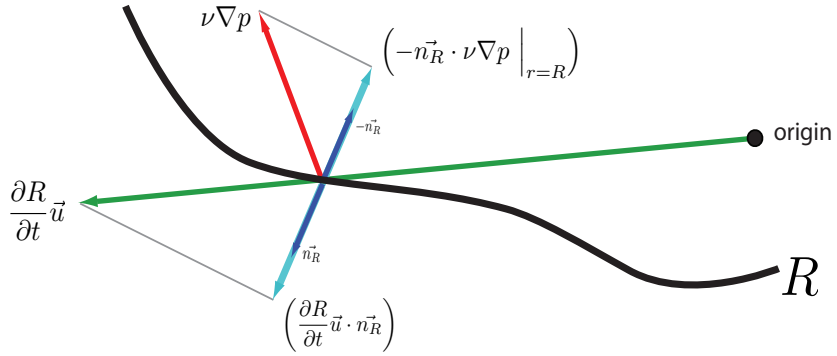

Figure 1: Diagram of a description of the boundary evolution

$$\Delta f = \frac{1}{r^2}\left(\frac{\partial}{\partial r}\left(r^2\frac{\partial f}{\partial r}\right) + \underbrace{\frac{1}{\sin\phi}\frac{\partial}{\partial\phi}\left(\sin\phi\frac{\partial f}{\partial\phi}\right) + \frac{1}{\sin^2\phi}\frac{\partial^2 f}{\partial\theta^2}}_{\text{angular part}}\right). \tag{19}$$

In this sense, the $\frac{1}{R}$ term makes the curvature higher if it is like a circle of radius R.

1.2 Difficulties

One issue with solving the PDE system is that inside that across the boundary we must solve parabolic equations, inside the boundary we must solve an elliptic equation, and then from those we can solve the hyperbolic equation that describes the tumor boundary. These are shown in Figure 2, and the order of solutions is outlined below:

- Update ODE (Body)
- Update Parabolic Equations (Chemicals)

- Solve Elliptic Equation (Pressure)
- Update Hyperbolic Equations (Boundary)

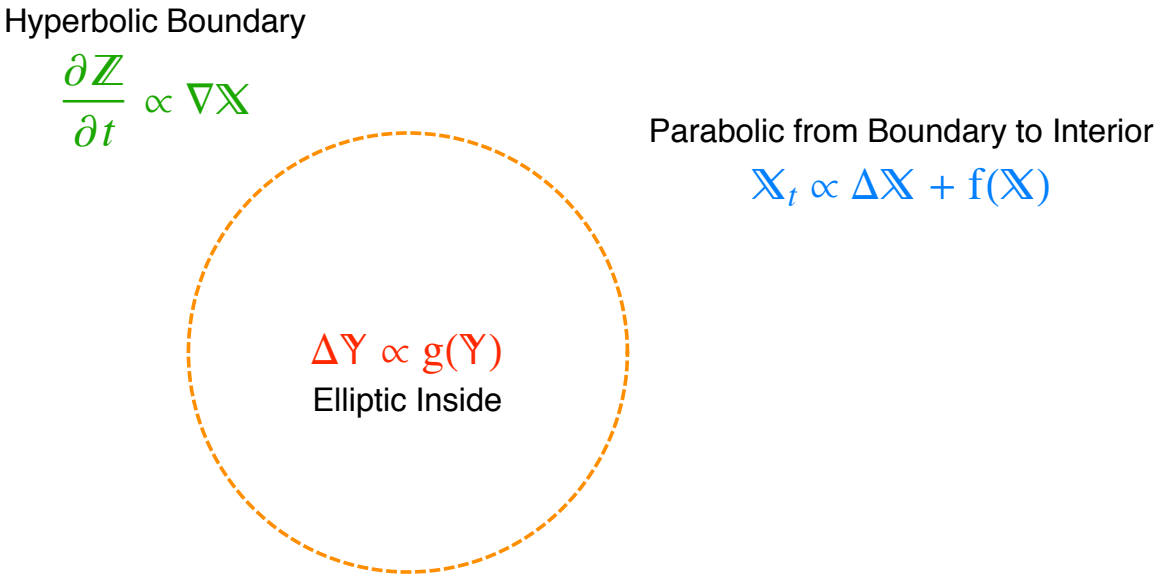

Figure 2: "Location" of PDE types in the spatial layout of our model

The challenge, then, of this scientific computing project is to implement a method to solve the elliptic equations inside the boundary very quickly, since they must be solved at each time step for whatever method we used to solve the time dependent equations.

2 Multi-Domain Spectral Method

A method from [1] has been used to solve Poisson's equation throughout a sphere using a multi-domain spectral approach. We essentially are trying to solve

$$\Delta F = S \tag{20}$$

where S is the source of some energy (like thermal or electric charge), and F is the potential set up by that source. The essence of the solution technique is as such:

- Project the source function onto spherical harmonics.
  This yields a sequence of radially dependent functions.
- Project the each radial function onto Chebyshev polynomials.
  This yields a sequence of coefficients.
- Invert a matrix that acts as the Laplace operator on the coefficients.
  This solves the equation.

- Un-transform the new coefficients into a radial function.
  This constructs our solutions out of spherical harmonics.
- Un-transform the new radial functions into a solution, namely F.
  This reconstructs the entire solution.

However, the initial source term may be piecewise radially defined from 0 to ∞. As such, each piece will denote a domain on which it is defined. The innermost of these domains will be the kernel, the outermost the external domain, and the remaining can be any number of shells including zero. We will first discuss the basis functions that we use for this approach, and then discuss the method for solving the system on each domain individually before stitching the solutions together to be continuous and have a continuous derivative along their boundary (if possible).

2.1 Basis Functions And Projections

We should review how to carry out the process of transformation to and from the spaces of the basis functions we are interested in projecting onto, and first we should review the structure of these functions.

2.1.1 Chebyshev Polynomials

Chebyshev polynomials are a family of orthogonal polynomials on $[-1, 1]$, and are eigenvalues of a differential equation, however the recurrence relation that defines

$$T_0(x) = 1 \quad T_1(x) = x \quad T_{n+1}(x) = 2xT_n(x) - T_{n-1}(x). \tag{21}$$

The polynomials generated from this relation are orthogonal under a "circular measure", i.e.,

$$(T_n, T_m) = \int_{-1}^{1} \frac{T_n T_m}{\sqrt{1-x^2}}\, dx = \frac{\pi}{2}(1 + \delta_{0n})\delta_{mn} \tag{22}$$

where $\delta_{ij} = 1$ if $i = j$, else $\delta_{ij} = 0$ if $i \neq j$. However, on the interval $[-1, 1]$, we can explicitly write

$$T_n(x) = \cos(n \cos^{-1}(x)). \tag{23}$$

With a change of variables given by

$$\theta = \cos^{-1}(x), \tag{24}$$

we can see that the orthogonality relation becomes

$$(T_n, T_m) = \int_{\pi}^{0} -\cos(n\theta)\cos(m\theta)\, d\theta = \int_{0}^{\pi} \cos(n\theta)\cos(m\theta)\, d\theta = \frac{\pi}{2}(1 + \delta_{0n})\delta_{mn} \tag{25}$$

Since we can, through a change of variables, turn integration against Chebyshev polynomials into integration against cosines, we can use a FFT to carry out a "Chebyshev Transform."

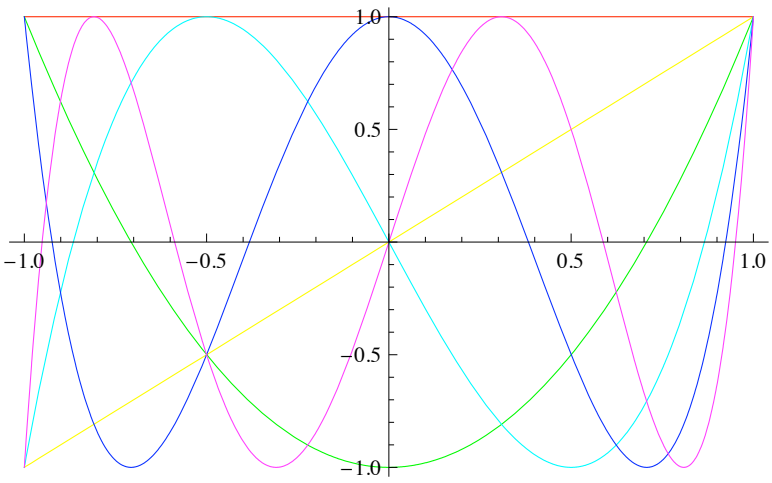

Figure 3: The first Chebyshev polynomials, from T_0 to T_5.

However, we must choose collocation points wisely, so as to exploit the full resolution allowed by the FFT. Our collocation points can include neither, one, or both of the endpoints of our interval, and to gain the full effectiveness of the FFT we choose Chebyshev-Gauss-Lobatto points which includes both endpoints for spacing, but we only use one of the endpoints during the FFT.

2.1.2 Spherical Harmonics

Sines and Cosines are the fundamental spatial solution to the heat equation. Fourier supposed that since they made up the fundamental solutions, they should be able to express all initial conditions, and so the Fourier Series expansion of a function was designed. The fundamental solutions the angular part of the Laplace operator are spherical harmonics, and as such they serve, in the natural way, as a basis upon which we can express all solutions to the angular part of Laplace's (or Poisson's equation).

These purely angular functions are given by

$$Y_\ell^m(\theta,\phi) = \sqrt{\frac{2\ell+1}{4\pi}\frac{(\ell-m)!}{(\ell+m)!}}P_\ell^m(\cos\phi)e^{im\theta} \tag{26}$$

where $\ell \geq 0$ and $|m| \leq m$. Often, the roles of ϕ and θ are reversed in the literature, depending on which field of study the spherical harmonics are discussed. The definition above (and how we will be using the spherical harmonics throughout this work), has ϕ as the elevation angle from the equator, and θ as the azimuthal angle from the prime meridian.

The P_ℓ^m in 26 are the associated Legendre polynomials, a family of orthogonal polynomials defined by

$$P_\ell^m(x) = \frac{(\ell+m)!}{(\ell-m)!}\frac{1}{2^\ell \ell!\sqrt{(1-x^2)^m}}\frac{d^{\ell-m}}{dx^{\ell-m}}\left(1-x^2\right)^2 \tag{27}$$

for $m \geq 0$, and

$$P_\ell^{-m}(x) = \frac{(\ell - m)!}{(\ell + m)!} P_\ell^m(x). \tag{28}$$

Like the spherical harmonics, the definition of the Legendre polynomials can vary in the literature, in this case having to do with the normalization factors.

2.2 Multiple Domains

As described above, we take on a multiple domain approach in our method of solution. The domains we may consider are diagrammed in Figure 4.

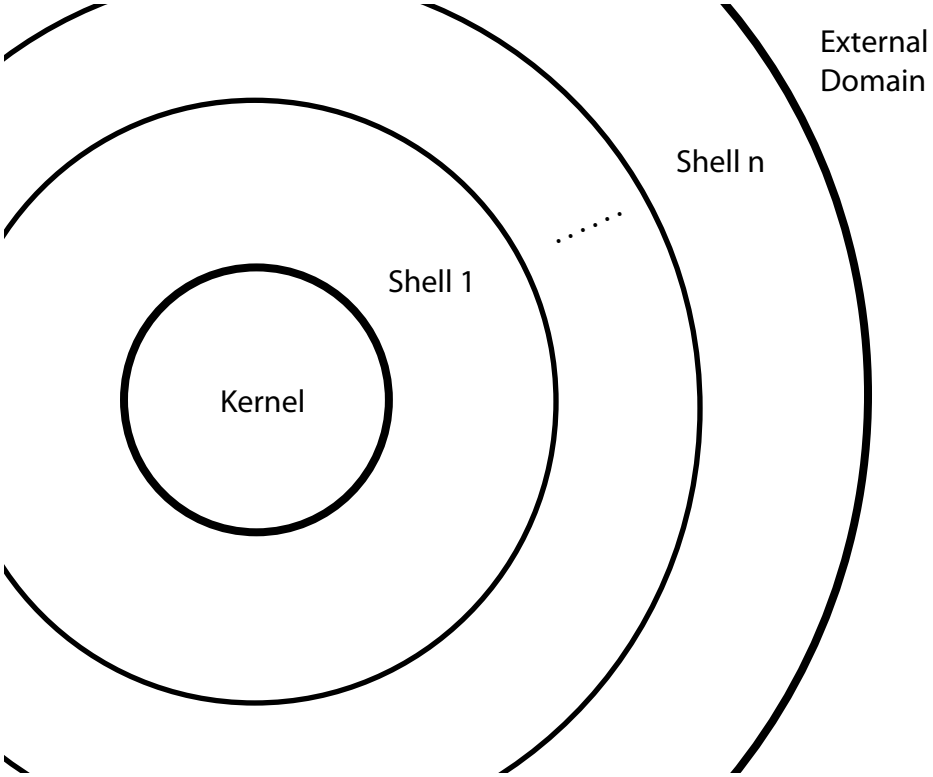

Figure 4: A diagram of the organization of the multiple domains, where n, the number of shells, is ≥ 0.

In each domain, we start with our source function, S, throughout the sphere, $S(r, \theta, \phi)$. We then use `MexS2kit`, a mex version of the C-code $S2kit$, to carry out the spherical harmonic transform, which yields

$$S(r, \theta, \phi) = \sum_{\ell=0}^{\ell_{\max}} \sum_{m=-\ell}^{\ell} s_{\ell m}(r) Y_\ell^m(\theta, \phi). \tag{29}$$

Then, for each (ℓ, m), we can use the coordinate transformation appropriate for the domain we are in and project the radial function $s_{\ell m}$ onto Chebyshev Polynomials via the FFT,

yielding

$$s_{\ell m}(x) = \sum_{n=0}^{n_{\max}} s_{\ell m}^n T_n(x). \tag{30}$$

Once we have the $s_{\ell m}^n$'s for each domain, we can put them in a vector, $S_{\ell m}$. The vector $F_{\ell m}$ is then a vector of the Chebyshev coefficients of the solution in that domain for that spherical harmonic, which is related to the coefficients in the source vector by a matrix operator, $A_{\ell m}$, by

$$A_{\ell m} F_{\ell m} = S_{\ell m}. \tag{31}$$

The coefficients of the A matrices can be computed by the orthogonality relations of Chebyshev polynomials in conjunction with the radial operator that we mean to solve, namely

$$\frac{d^2 f_{\ell m}(r)}{dr^2} + \frac{2}{r}\frac{df_{\ell m}(r)}{dr} - \frac{\ell(\ell+1) f_{\ell m}(r)}{r^2} = s_{\ell m}(r). \tag{32}$$

Once we have solved the system, we can pass the coefficients in $F_{\ell m}$ through the reverse Chebyshev transform to get $f_{\ell m}(r)$, and then pass all of the radial function through the reverse spherical harmonic transform to get $F(r, \theta, \phi)$ in each domain.

2.3 Stitching

A certain amount of care must be taken when solving the matrix system so as to allow for the solutions in the individual domains to be matched for continuity and continuity of derivatives. In short, the matrices are stripped of the leftmost rows and bottommost columns that correspond to the zero eigenvalue of the matrix. With respect to the differential operator, these rows and columns correspond to the homogenous solutions to Equation 32.

Because we have removed them when we solve the system, our solution is underdetermined. However, this allows us to created the fully determined system by solving for the coefficients of the homogeneous solutions for all of the domains together, which allows us to stitch the solutions from the domains together in the way that we'd want to.

3 Conclusions

While the work as a whole in [1] can be used to solve the pressure equation in our tumor model, it has not as of yet in this project. The analytical examples against which one can test the implementation of [1] should test four things: spherically symmetric solutions in the kernel and external domains, spherically asymmetric solutions in the kernel and external domains, stitching asymmetric solutions through multiple shells, pointwise convergence in cases where Gibbs phenomenon is exhibited. The four analytical examples given in the paper test for these precisely.

3.1 Results

The main result of this project is an implementation of the transformations of the data that must occur, and a spectral solution of the spherically symmetric case. Additionally, a full MATLAB code architecture is incorporated into the `gbFinal` code included with this document which is ready to solve the asymmetric, multi-shell, and Gibbs cases. However, certain issues with the numerical methods used in our approach have yield only unsuccessful attempts.

Figure 5 shows the analytical and computed solution for the spherically symmetric case for a low amount of Chebyshev coefficients, using a singular operator (the r^4 method) in the external domain, and we can see that even at these low numbers we have achieved spectral accuracy. These results are actually better than reported in [1], which is confusing. However, these results may be explained through the use of an FFT and more appropriate collocation points than in [1].

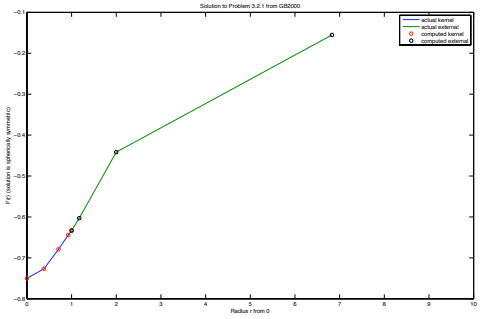

Figure 5: Symmetric case, $n_{\max} = 4, \ell_{\max} = 0$

Figure 6 shows that for more points using the r^4 method that the numerical solution is stable.

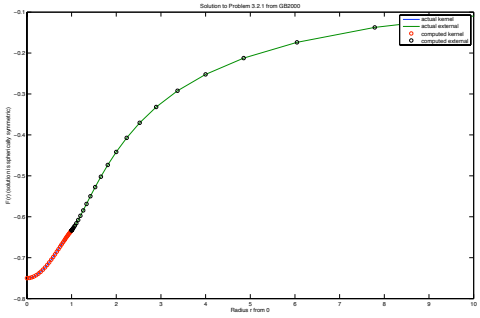

Figure 6: Symmetric case, $n_{\max} = 30, \ell_{\max} = 0$

Figure 7 shows that using a non-singular operator in the external domain (the r^2 method), we do not resolve the correct solution for the external domain.

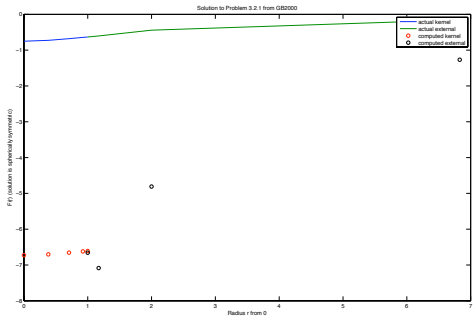

Figure 7: Symmetric case, $n_{\max} = 4, \ell_{\max} = 0$

Figure 8 shows that for more points we converge on the incorrect solution from 7.

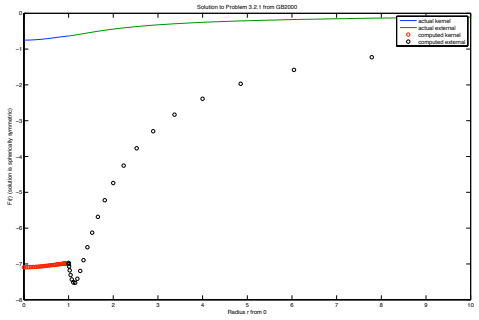

Figure 8: Symmetric case, $n_{\max} = 30, \ell_{\max} = 0$

Figure 9 shows that for even more points, the iterative solver used to invert the matrix operators converges to a different solution, which is still not particularly helpful.

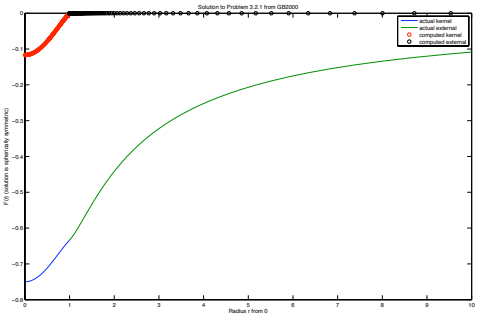

Figure 9: Symmetric case, $n_{\max} = 70, \ell_{\max} = 0$

Figure 10 show that for the symmetric spherical harmonic part of the asymmetric problem, we find the correct solution in the kernel, but not in the external domain.

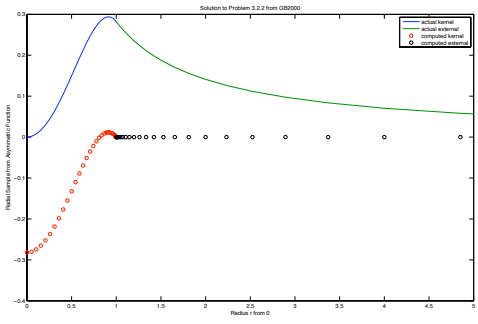

Figure 10: Asymmetric case, $n_{\max} = 30, \ell_{\max} = 0$

Figure 11 shows that we are converging on a nice solution for the symmetric part of the problem.

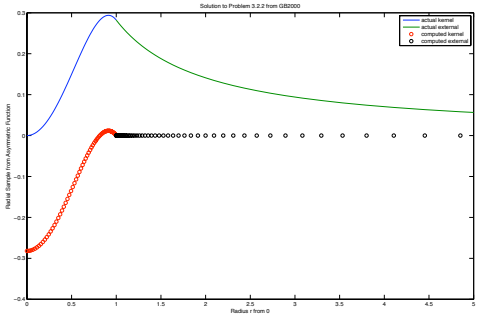

Figure 11: Asymmetric case, $n_{\max} = 70, \ell_{\max} = 0$

Figure 12 show that when we try and solve for higher order spherical harmonics, even our solution in the kernel is begins to vary.

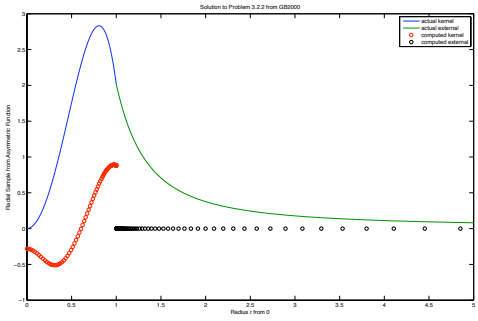

Figure 12: Asymmetric case, $n_{\max} = 70, \ell_{\max} = 3$

Figure 13 show that adding more spherical harmonics to the decomposition adds even

more polynomial oscillations to our kernel solution.

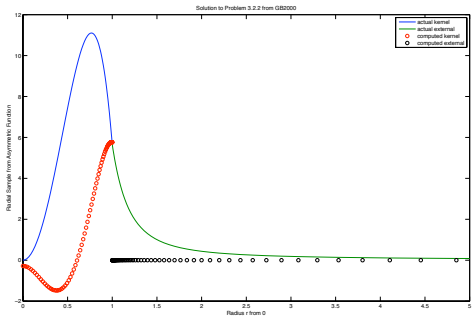

Figure 13: Asymmetric case, $n_{\max} = 70, \ell_{\max} = 7$

3.2 Issues

The issues that become apparent while implementing the method in [1] revolve around solving the matrix system. The matrices used to represent the operators of interested of very badly conditioned, and as such iterative methods must be used to find good candidates for their inverses. These iterative methods are good in most cases, however, the structure of some of the matrices we are interested in using are elusive, if not simply incorrect. Possibly a future iteration of the work done here might yield some insight as to how to address the issue.

3.3 Future Work

In order to complete the task of solving Poisson's equation quickly so as to apply its solution in our tumor model, future work includes:

- completing the implementation of the multi-domain spectral method in [1],
- extending the implementation to include a moving spherical boundary and to incorporate time-dependent, internally diffusing molecules into the source term for the elliptic equation at each time step, and
- extending the implementation to include a moving non-spherical boundary.

In short, the work presented in [1] shows great promise in aiding cancer modeling, however, its implementation has proven difficult and intricate in unexpected ways.

References

[1] P. Grandclement, S. Bonazzola, E. Gourgoulhon, J.-A. Marck. "*A multi-domain spectral method for scalar and vectorial Poisson equations with non-compact sources*".

J.Comput.Phys. 170 (2001) 231-260. Available at: http://arxiv.org/abs/gr-qc/0003072v2